4 GRIN Lenses for Gaussian Illumination

4.1 Introduction

In Chap. 3, we discussed behavior of GRIN lenses illuminated by a uniform monochromatic wave. But, it is well–known that the output modes of most lasers can be simply described by Hermite–Gaussian or Laguerre–Gaussian functions. Therefore, for applications involving the propagation of laser beams, it is important to understand the effect of GRIN lenses on such Gaussian beams since these lenses are used, for instance, in optical fiber communications and optoelectronic systems for manipulating and processing optical signals.

Chapter 4 summarizes some useful properties of Gaussian beams and studies the laws of transformation of these beams through and by GRIN lenses. Chapter 4 also discusses other related topics for non–uniform monochromatic waves described by Gaussian beams.

4.2 Propagation of Gaussian Beams in a GRIN Lens

We consider a GRIN lens with rotational symmetry around the z–axis whose refractive index is given by Eq. (3.1). We shall now study light propagation in a GRIN lens when it is illuminated by a non-uniform monochromatic wave of wavelength λ, described by a Gaussian beam. That is, we are concerned with waves whose irradiance is maximum on the axis and decreases as a Gaussian function with distance from the axis. This is why the waves are called Gaussian beams. These beams are solutions of the scalar parabolic wave equation, and they are represented by the Hermite–Gauss or Laguerre–Gauss modes of lowest–order [4.1].

When a GRIN lens is illuminated, for instance, by a spherical Gaussian beam (Fig. 4.1), the complex amplitude at the input face can be written in the paraxial region by [4.2–4.4]

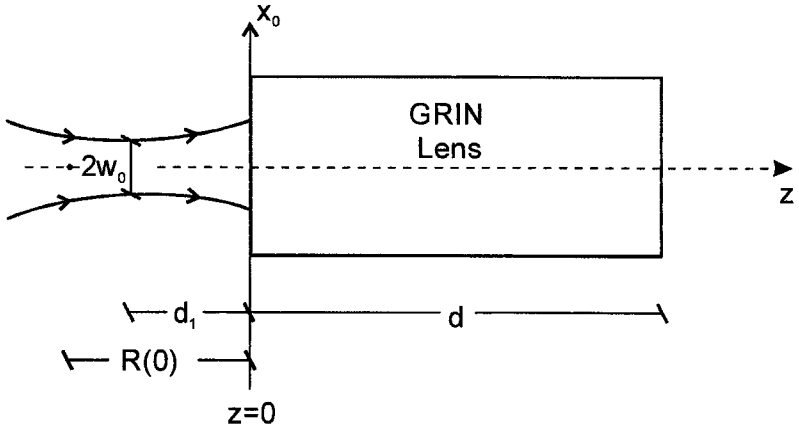

Fig. 4.1. Geometry for the evaluation of the complex amplitude distribution inside a GRIN lens illuminated by a Gaussian beam, where R(0), w_0, and d_1 are the curvature radius, the beam waist, and the distance from the waist plane to the input face of the GRIN lens, respectively.

$$\psi(x_0, y_0; 0) = \frac{w_0}{w(0)} \exp\{i\varphi(0)\} \exp\left\{ i \frac{\pi U(0)}{\lambda} \left(x_0^2 + y_0^2\right) \right\} \tag{4.1}$$

where the beam parameters in free space at a distance d_1 from the waist plane of diameter or spot size $2w_0$ are given by the complex wavefront curvature

$$U(0) = \frac{1}{R(0)} + i \frac{\lambda}{\pi w^2(0)} \tag{4.2}$$

and the on–axis phase

$$\varphi(0) = -\tan^{-1}\left(\frac{\lambda d_1}{\pi w_0^2} \right) \tag{4.3}$$

where R(0) and w(0) are the radius of curvature and the beam half–width or beam radius at $z = 0$. The beam half–width is the distance from the axis at which the irradiance decays to e^{-2} of its maximum value [4.5]. Complex wavefront curvature reduces to real wavefront curvature in the geometrical optics limit, $k \to \infty$.

Likewise, the relationship between the beam radius at $z = 0$ and the waist radius is governed by

$$w(0) = w_0 \left[1 + \left(\frac{d_1}{z_0} \right)^2 \right]^{1/2} \tag{4.4}$$

where

$$z_0 = \frac{\pi w_0^2}{\lambda} \tag{4.5}$$

is the Rayleigh range characterizing the Lorentzian profile of irradiance along the axis.

The complex amplitude distribution in the GRIN lens is given by the integral transform from Eq. (2.1)

$$\psi(x,y;z) = \int_{\Re^2} \psi(x_0,y_0;0)K(x_0,y_0,x,y;z)\,dx_0dy_0 \tag{4.6}$$

where K is the kernel function.

Substituting Eq. (4.1) into Eq. (4.6) and integrating, we have

$$\psi(x,y;z) = \frac{w_0}{w(0)G(z)}\exp\{i\varphi(z)\}\exp\left\{\frac{i\pi n_0\dot{G}(z)}{\lambda G(z)}(x^2+y^2)\right\} \tag{4.7}$$

where Eq. (2.20) has been used.

Equation (4.7) is the central result of the present analysis, and it represents a spherical Gaussian beam of complex curvature.

$$U(z) = n_0\frac{d}{dz}[\ln G(z)] = n_0\dot{G}(z)G^{-1}(z) \tag{4.8}$$

and the on–axis phase

$$\varphi(z) = \varphi(0) + kn_0z \tag{4.9}$$

where

$$\overset{(\cdot)}{G}(z) = \overset{(\cdot)}{H}_f(z) + \frac{U(0)}{n_0}\overset{(\cdot)}{H}_a(z) \tag{4.10}$$

The complex curvature may also be expressed as [4.6]

$$U(z) = \frac{1}{R(z)} + i\frac{\lambda}{\pi w^2(z)} \tag{4.11}$$

where R(z) and w(z) are the radius of curvature and the beam half–width of the Gaussian beam in the GRIN lens at z.

When Eq. (4.8) is compared with Eq. (4.11) and Eqs. (4.2) and (4.10) are taken into account, it follows that R(z) and w(z) are given by

$$\begin{aligned}\frac{1}{R(z)} = \frac{1}{|G(z)|^2}\Bigg\{&\frac{1}{R(0)}\left[H_a(z)\dot{H}_f(z) + \dot{H}_a(z)H_f(z)\right] \\ &+\left[\frac{1}{z_R^2} + \frac{1}{n_0^2R^2(0)}\right]n_0H_a(z)\dot{H}_a(z) + n_0H_f(z)\dot{H}_f(z)\Bigg\}\end{aligned} \tag{4.12}$$

$$w^2(z) = w^2(0)|G(z)|^2 \tag{4.13}$$

where z_R is the Rayleigh range along the z–axis of the GRIN lens, expressed as

$$z_R = \frac{\pi n_0 w^2(0)}{\lambda} \tag{4.14}$$

and $|G|$ is the modulus of G(z); that is

$$|G(z)|^2 = \left[\frac{H_a(z)}{n_0 R(0)} + H_f(z)\right]^2 + \frac{H_a^2(z)}{z_R^2} = G_r^2(z) + G_i^2(z) \tag{4.15}$$

which relates the beam radius at $z > 0$ to the beam radius at the input face of the GRIN lens, where G_r and G_i are the real and imaginary parts of G, respectively.

Likewise, from Eqs. (4.8) and (4.13) it follows that the complex amplitude distribution of the Gaussian beam in the GRIN lens can be written as

$$\psi(x,y;z) = \frac{w_0}{w(z)} \exp\{i\varphi(z)\} \exp\left\{-i\tan^{-1}\left[G_i(z)/G_r(z)\right]\right\} \exp\left\{i\frac{\pi U(z)}{\lambda}(x^2+y^2)\right\} \tag{4.16}$$

Equations (4.7) or (4.16) include plane Gaussian illumination as a particular case. For this illumination, the waist w_0 is located at the input face of the GRIN lens and $R(0) \to \infty$. Under these conditions $\overset{(\cdot)}{G}(z)$ becomes

$$\overset{(\cdot)}{G}_p(z) = \overset{(\cdot)}{H}_f(z) + i\frac{\overset{(\cdot)}{H}_a(z)}{z_{pR}} \tag{4.17}$$

where

$$z_{pR} = \frac{\pi n_0 w_0^2}{\lambda} \tag{4.18}$$

and the radius of curvature, beam profile, and complex amplitude distribution for plane illumination are now given by

$$\frac{1}{R_p(z)} = \frac{n_0}{|G_p(z)|^2}\left[\frac{H_a(z)\dot{H}_a(z)}{z_{pR}^2} + H_f(z)\dot{H}_f(z)\right] \tag{4.19}$$

$$w_p^2(z) = w_0^2 |G_p(z)|^2 \tag{4.20}$$

$$\psi_p(x,y;z) = \frac{1}{|G_p(z)|} \exp\{i\varphi_p(z)\} \exp\left\{-i\tan^{-1}\left[\frac{H_a(z)}{z_{pR}H_f(z)}\right]\right\} \exp\left\{i\frac{\pi U_p(z)}{\lambda}(x^2+y^2)\right\} \tag{4.21}$$

where

$$\varphi_p(z) = kn_0 z - \tan^{-1}\left(\frac{n_0 d_1}{z_{pR}}\right) \tag{4.22}$$

$$U_p(z) = n_0 \dot{G}_p(z) G_p^{-1}(z) \tag{4.23}$$

On the other hand, as mentioned in Chap. 2, there is a connection between the kernel function and the ray–transfer matrix that leads to useful relations between the geometrical ray optics and the wave optics. In this way, the passage of a Gaussian beam through a GRIN lens is described by the ABCD law [4.7]

$$\begin{pmatrix} q(z) \\ n_0\dot{q}(z) \end{pmatrix} = \begin{pmatrix} A' & B' \\ C' & D' \end{pmatrix} \begin{pmatrix} q(0) \\ n_0\dot{q}(0) \end{pmatrix} \tag{4.24}$$

where the elements of the ray–transfer matrix are given by Eqs. (1.91b).

In this case, the ABCD law relate complex rays whose positions and optical direction cosines are denoted by $q(0)$, $n_0\dot{q}(0)$ and q, $n_0\dot{q}$ at the planes $z = 0$ and $z > 0$, respectively. The complex parameters q and $\dot{q}$, resulting from real rays by means of analytic continuation, describe Gaussian beam propagation and play a role similar to the one played by the position and slope of the real geometrical rays used in uniform illumination.

The complex beam parameter $q(z)$ obeys the paraxial ray equation, and the real and imaginary parts q_r and q_i, respectively, are also two solutions of the equation [4.1, 4.2]

$$\ddot{q}_{\binom{r}{i}} + g^2(z)q_{\binom{r}{i}} = 0 \tag{4.25}$$

satisfying the z–invariant condition

$$q_r\dot{q}_i - \dot{q}_r q_i = \frac{2}{kn_0} \tag{4.26}$$

or equivalently

$$q^*\dot{q} - q\dot{q}^* = 2i(q_r\dot{q}_i - \dot{q}_r q_i) = \frac{4i}{kn_0} \tag{4.27}$$

In order to find the relations between the geometrical ray optics and the wave optics for Gaussian beam propagation in a GRIN lens, Eq. (4.24) is written as

$$q(z) = q(0)[A' + n_0\dot{q}(0)q^{-1}(0)B'] \tag{4.28a}$$

$$\dot{q}(z) = q(0)\left[\frac{C'}{n_0} + \dot{q}(0)q^{-1}(0)D'\right] \tag{4.28b}$$

At the input face of the GRIN lens, position and slope of the complex rays are given by

$$q(0) = w_0 + i\frac{\lambda d_i}{\pi w_0} \tag{4.29a}$$

$$\dot{q}(0) = \frac{i\lambda}{\pi w_0 n_0} \tag{4.29b}$$

From Eqs. (4.29) and after straightforward calculation we obtain

$$n_0\dot{q}(0)q^{-1}(0) = U(0) \tag{4.30}$$

where the following relationship

$$R(0) = d_1\left[1+\left(\frac{\pi w_0^2}{\lambda d_1}\right)^2\right] \tag{4.31}$$

between R(0) and d_1 has been used, and U(0) is given by Eq. (4.2).

Substitution of Eq. (4.30) into Eqs. (4.28) provides

$$q(z) = q(0)G(z) \tag{4.32a}$$

$$\dot{q}(z) = q(0)\dot{G}(z) \tag{4.32b}$$

where $\overset{(\cdot)}{G}(z)$ coincides with Eq. (4.10). Then, from Eqs. (4.32) the complex curvature of the Gaussian beam in the GRIN lens can be now expressed in terms of q(z) and $\dot{q}(z)$ as

$$U(z) = n_0\dot{q}(z)q^{-1}(z) \tag{4.33}$$

that is, U(z) in terms of the ray matrix elements is written as [4.8–4.14].

$$U(z) = \frac{C' + U(0)D'}{A' + U(0)B'} \tag{4.34}$$

Comparing Eq. (4.33) with Eq. (4.11), the beam half–width and the radius of curvature of the Gaussian beam in terms of q and $\dot{q}$ are given by

$$w^2(z) = \frac{\lambda|q(z)|^2}{n_0\pi[q_r(z)\dot{q}_i(z) - \dot{q}_r(z)q_i(z)]} = |q(z)|^2 \tag{4.35}$$

$$\frac{1}{R(z)} = \frac{n_0[q_r(z)\dot{q}_r(z) + q_i(z)\dot{q}_i(z)]}{|q(z)|^2} = \frac{n_0}{|q(z)|}\frac{d|q(z)|}{dz} = n_0\frac{d}{dz}\ln|q(z)| \tag{4.36}$$

where Eq. (4.26) has been used.

From Eqs. (4.35-38) it follows that the modulus of the complex ray is equal to the beam half-width and that R(z) and w(z) are related by

$$\frac{1}{R(z)} = \frac{n_0}{2w^2(z)}\frac{dw^2(z)}{dz} \tag{4.37}$$

Finally, the on-axis phase of Eq. (4.16) in terms of the complex ray may be expressed as [4.2]

$$kn_0 z - \frac{1}{2}\,\text{phase}\left[\frac{q(z)}{q(0)}\right] = kn_0 z + \frac{1}{2}\tan^{-1}\left[\frac{q_i(0)}{q_r(0)}\right] - \frac{1}{2}\tan^{-1}\left[\frac{q_i(z)}{q_r(z)}\right] \tag{4.38}$$

$$= kn_0 z + \frac{1}{2}\tan^{-1}\left\{\frac{1}{q_r(0)q_r(z) + q_i(0)q_i(z)}\left[\frac{q_i(0)}{q_r(0)} - \frac{q_i(z)}{q_r(z)}\right]\right\}$$

In short, the wave optics parameters (complex wavefront curvature and on–axis phase) defining the field of a Gaussian beam can be related, in a simple way, to the complex ray q.

Equation (4.13) indicates the evolution of the half-width; we are now interested in those lengths where the half–width is an extremum (beam waist). Then, the condition of the plane Gaussian beam inside the GRIN lens can be obtained by evaluation of the extremum values of the beam half-width or by the vanishing of the wavefront curvature. From Eq. (4.13) or (4.37), this condition provides

$$\frac{dw^2(z)}{dz} = \frac{d|G(z)|^2}{dz} = 0 \tag{4.39}$$

that is,

$$\frac{1}{R(0)}\left[H_a(z)\dot{H}_f(z) + \dot{H}_a(z)H_f(z)\right] + \left[\frac{1}{z_R^2} + \frac{1}{n_0^2 R^2(0)}\right] n_0 H_a(z)\dot{H}_a(z) + n_0 H_f(z)\dot{H}_f(z) = 0 \tag{4.40}$$

where Eqs. (4.12) or (4.15) have been used.

Equation (4.40) has two oscillatory solutions z^+ and z^-, in which the beam half–width can be a maximum or a minimum. The axial localizations of these positions can be obtained if we take into account that position and slope of the axial and field rays, given by Eqs. (1.92) and (1.95), are written as

$$H_a(z) = -\frac{\dot{H}_f(z)}{g_0 g(z)} = \frac{u(z)}{\{g_0 g(z)[1 + u^2(z)]\}^{1/2}} \tag{4.41}$$

$$H_f(z) = \frac{g_0}{g(z)}\dot{H}_a(z) = \left\{\frac{g_0}{g(z)[1 + u^2(z)]}\right\}^{1/2} \tag{4.42}$$

where

$$u(z) = \tan\left[\int_0^z g(z')\,dz'\right] \tag{4.43}$$

Substituting Eqs. (4.41, 4.42) into Eq. (4.40), we have the following second-order equation

$$au^2(z) + bu(z) + c = 0 \tag{4.44}$$

with

$$a = -c = \frac{g_0}{R(0)} \tag{4.45a}$$

$$b = -n_0\left[\frac{1}{z_R^2} + \frac{1}{n_0^2 R^2(0)} - g_0^2\right] \tag{4.45b}$$

Taking into account Eq. (4.14), solution of Eq. (4.44) is given by

$$u(z^{\pm}) = \frac{n_0}{2g_0}\left\{\frac{1}{n_0^2 R(0)} + g_0^2 R(0)\left[\frac{w_{fm}^4(0)}{w^4(0)} - 1\right]\right\} \pm \left\{\left(\frac{n_0}{2g_0}\right)^2\left[\frac{1}{n_0^2 R(0)} + g_0^2 R(0)\left[\frac{w_{fm}^4(0)}{w^4(0)} - 1\right]\right]^2 + 1\right\}^{1/2} \tag{4.46}$$

where

$$w_{fm}(0) = \left(\frac{\lambda}{\pi n_0 g_0}\right)^{1/2} \tag{4.47}$$

is the half–width of the fundamental mode at z = 0 in a tapered GRIN medium [4.15], and with the use of plus for z^+ and minus for z^-. Note that when $w_{fm}(0) = w(0)$, it follows from Eq. (4.46) that the axial positions of extremum values of the beam half–width reduces to

$$u_p(z^{\pm})\big|_{w_{fm}(0)=w(0)} = \frac{1}{2n_0 g_0 R(0)} \pm \left[\left(\frac{1}{2n_0 g_0 R(0)}\right)^2 + 1\right]^{1/2} \tag{4.48}$$

On the other hand, $|G(z)|$ given by Eq. (4.15) can be expressed in terms of u(z) as

$$|G(z)|^2 = \frac{g_0}{g(z)[1+u^2(z)]}\left[\left(\frac{u(z)}{n_0 g_0 R(0)} + 1\right)^2 + \frac{u^2(z) w_{fm}^4(0)}{w^4(0)}\right] \tag{4.49}$$

and the second derivative of Eq. (4.49) with respect to z is given by

$$\frac{d^2|G(z)|^2}{dz^2} = \frac{2g(z)}{n_0[1+u^2(z)]} \cdot\left\{-4\frac{u(z)}{R(0)} + \frac{n_0}{g_0}\left[1-u^2(z)\right]\left[\frac{1}{n_0^2 R_0^2} + g_0^2\left(\frac{w_{fm}^4(0)}{w^4(0)} - 1\right)\right]\right\} \tag{4.50}$$

It is easy to prove that when $w_{fm}(0)$ is greater than, smaller than, or equal to w(0) and R(0) > 0 (diverging illumination), we have

$$\left.\frac{d^2|G(z)|^2}{dz^2}\right|_{u(z)=u(z^+)} \langle 0, \text{ and } \left.\frac{d^2|G(z)|^2}{dz^2}\right|_{u(z)=u(z^-)} \rangle 0 \tag{4.51}$$

Then, the axial positions in which the beam half-width is a maximum or a minimum are given by $u(z^+)$ and $u(z^-)$, respectively.

Conversely, when $w_{fm}(0)$ is greater than, smaller than, or equal to w(0) and R(0)<0 (converging illumination), we arrive at

$$\left.\frac{d^2|G(z)|^2}{dz^2}\right|_{u(z)=u(z^+)} \rangle 0, \text{ and } \left.\frac{d^2|G(z)|^2}{dz^2}\right|_{u(z)=u(z^-)} \langle 0 \tag{4.52}$$

The axial locations in which the beam half–width is a maximum or a minimum are obtained for $u(z^-)$ and $u(z^+)$, respectively.

Likewise, it is also of interest to examine the evolution of the beam half–width for plane Gaussian illumination. In this case, for $w_{fm} \langle w_0$ and $w_{fm} \rangle w_0$, Eqs. (4.50) and (4.46) become

$$\left.\frac{d^2|G(z)|^2}{dz^2}\right|_{R(0)\to\infty} = \frac{2g(z)g_0[1-u^2(z)]}{1+u^2(z)}\left\{\frac{w_{fm}^4(0)}{w_0^4}-1\right\} \tag{4.53}$$

$$\lim_{R(0)\to\infty} u(z^+) \to \begin{cases} \infty & \text{for } w_{fm}(0) \rangle w_0 \\ 0 & \text{for } w_{fm}(0) \langle w_0 \end{cases} \tag{4.54}$$

$$\lim_{R(0)\to\infty} u(z^-) \to \begin{cases} 0 & \text{for } w_{fm}(0) \rangle w_0 \\ -\infty & \text{for } w_{fm}(0) \langle w_0 \end{cases} \tag{4.55}$$

From Eqs. (4.54–4.55) and (4.43) it follows that when $w_{fm} \rangle w_0$, we have

$$\cos\left[\int_0^{z^+} g(z')dz'\right] = 0 \text{ or } H_f(z^+) = 0, \text{ for } u(z^+) \tag{4.56}$$

$$\sin\left[\int_0^{z^-} g(z')dz'\right] = 0 \text{ or } H_a(z^-) = 0, \text{ for } u(z^-) \tag{4.57}$$

where Eqs. (1.92) have been used.

For Gaussian plane illumination and $w_{fm}(0) \rangle w_0$, the sign of the second derivative of |G(z)| evaluated at $u(z^\pm)$ is given by

$$\left.\frac{d^2|G(z)|^2}{dz^2}\right|_{u(z)=u(z^+)} \langle 0 \tag{4.58}$$

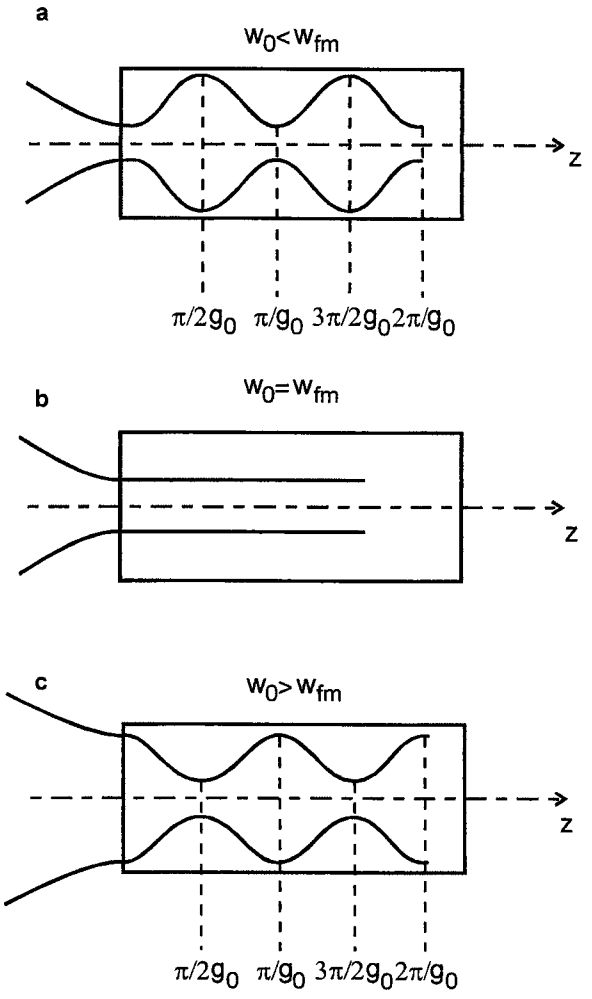

Fig. 4.2. Evolution of the beam half-width inside a selfoc lens illuminated by a plane Gaussian beam for **a** $w_{fm} > w_0$, **b** $w_{fm} = w_0$, and **c** $w_{fm} < w_0$.

$$\left.\frac{d^2|G(z)|^2}{dz^2}\right|_{u(z)=u(z^-)} \rangle 0 \tag{4.59}$$

Consequently, the maximum or minimum values of the beam half-width are achieved at the transforming and imaging conditions respectively, as mentioned in Chap. 2. The reverse behavior occurs for Gaussian plane illumination and $w_{fm}(0) \langle w_0$.

Finally, note that when $w_{fm}(0) = w_0$, it follows from Eqs. (4.49) and (4.53) that

$$|G(z)|^2_{\substack{R(0)\to\infty \\ w_{fm}(0)=w_0}} = \frac{g_0}{g(z)} \tag{4.60}$$

$$\left.\frac{d^2|G(z)|^2}{dz^2}\right|_{\substack{R(0)\to\infty \\ w_{fm}(0)=w_0}} = 0 \tag{4.61}$$

for all values of z inside the GRIN lens, and the incident plane Gaussian beam propagates as the fundamental mode since

$$w(z)|_{\substack{R(0)\to\infty \\ w_{fm}(0)=w_0}} = \left[\frac{g_0}{g(z)}\right]^{1/2} w_{fm}(0) = \left[\frac{\lambda}{\pi n_0 g(z)}\right]^{1/2} = w_{fm}(z) \tag{4.62}$$

where Eqs. (4.20) and (4.47) have been used.

Figure 4.2 depicts the evolution of the beam half-width inside a selfoc lens illuminated by a plane Gaussian beam. When $w_{fm} = w_0$ the beam propagates as the fundamental mode, and there is an adiffractional Gaussian beam inside the selfoc lens.

4.3 GRIN Lens Law: Image and Focal Shifts

We now consider transformation of Gaussian beams by a GRIN lens. Referring to the geometry of Fig. 4.3, and in comparison to the uniform illumination case in calculating the GRIN lens law, we regard the waist of the input beam as the object, and the waist of the output beam as the image. The ratio of the input waist to the output waist is the transverse magnification. Our aim is to determine the condition for which the output beam radius becomes the output waist, that is, for which the beam half-width is a minimum.

We apply the ABCD law to the derivation of the GRIN lens law for Gaussian beams. The ray position q' and the ray slope $\dot{q}'$ at any output plane of the optical system, located at distance d' from the output face of the GRIN lens, are related by the ray position q_0 and slope $\dot{q}_0$ at the waist w_0 of the input Gaussian beam by the matrix equation

$$\begin{pmatrix} q' \\ \dot{q}' \end{pmatrix} = M_s \begin{pmatrix} q_0 \\ \dot{q}_0 \end{pmatrix} \tag{4.63}$$

where

$$q_0 = w_0 \; ; \; \dot{q}_0 = \frac{i\lambda}{\pi w_0} \tag{4.64}$$

and the elements of the ray–transfer matrix M_s of the optical system are given by Eqs. (3.51) for $n_1 = n_1' = 1$, provided that the GRIN lens is surrounded by free space.

From Eqs. (3.51) and (4.63–4.64) it follows that

$$q' = w_0\left\{H_f(d) + n_0 d'\dot{H}_f(d) + \frac{i}{z_R}\left[H_a(d) + n_0 d'\dot{H}_a(d) + n_0 d_1\left(H_f(d) + n_0 d'\dot{H}_f(d)\right)\right]\right\} \tag{4.65}$$

Then the beam half–width of the Gaussian wavefront at the output plane can be written as

$$w' = |q'| = w_0\left\{\left[H_f(d) + n_0 d'\dot{H}_f(d)\right]^2 + \frac{1}{z_r^2}\left[H_a(d) + n_0 d'\dot{H}_a(d) + n_0 d_1\left(H_f(d) + n_0 d'\dot{H}_f(d)\right)\right]^2\right\}^{1/2} \tag{4.66}$$

The output beam half-width reaches its minimum value at the waist (Fig. 4.3). Thus, the image condition can be expressed as

$$\frac{dw'^2}{dd'} = 0 \tag{4.67}$$

Equation (4.67) indicates that the distance from the output face of the GRIN lens to the waist is given by [4.16].

$$\begin{aligned} d_g' &= -\frac{H_f(d)\dot{H}_f(d)z_R^2 + \left[\dot{H}_a(d) + n_0 d_1\dot{H}_f(d)\right]\left[H_a(d) + n_0 d_1 H_f(d)\right]}{n_0\left[\dot{H}_f^2(d)z_R^2 + \left(\dot{H}_a(d) + n_0 d_1\dot{H}_f(d)\right)^2\right]} \\ &= \frac{1}{2n_0 g^2(d)}\frac{d}{dz}\left\{\ln\left[\dot{H}_f^2(z)z_R^2 + \left(\dot{H}_a(z) + n_0 d_1\dot{H}_f(z)\right)^2\right]\right\}_{z=d} \end{aligned} \tag{4.68}$$

Equation (4.68) represents the final result of the present analysis and can be called the GRIN lens law for Gaussian illumination.

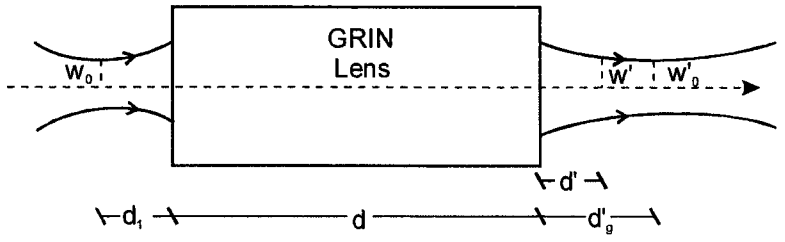

Fig. 4.3. Gaussian beam transformation by a GRIN lens.

Substituting Eq. (4.68) into Eq. (4.66), we obtain the waist of the output beam

$$w_0' = \frac{w_0}{\left[\dot{H}_f^2(z)z_R^2 + \left(\dot{H}_a(d) + n_0 d_1 \dot{H}_f(d)\right)^2\right]^{1/2}} \tag{4.69}$$

Then, the transverse magnification is given by

$$m_t^g = \frac{w_0'}{w_0} = \left[\dot{H}_f^2(z)z_R^2 + \left(\dot{H}_a(d) + n_0 d_1 \dot{H}_f(d)\right)^2\right]^{-1/2} \tag{4.70}$$

On the other hand, from the GRIN lens law we can also obtain the back working distance of the lens for Gaussian illumination, that is, the back focal length measured from the output face of the GRIN lens. The back working distance results when the incident beam has its waist located on the input face of the GRIN lens. At this particular case $d_1 = 0$, $z_R = z_{pR}$, and Eq. (4.68) becomes

$$\begin{aligned} l_g' &= -\frac{H_f(d)\dot{H}_f(d)z_{pR}^2 + H_a(d)\dot{H}_a(d)}{n_0\left[\dot{H}_f^2(d)z_{pR}^2 + \dot{H}_a^2(d)\right]} \\ &= \frac{1}{2n_0 g^2(d)}\frac{d}{dz}\ln\left[\dot{H}_f^2(z)z_{pR}^2 + \dot{H}_a^2(z)\right]\Big|_{z=d} \end{aligned} \tag{4.71}$$

Equation (4.71) reduces to the back working distance for uniform illumination, Eqs. (3.33) or (3.60), when $z_{pR} \to \infty$.

An example of the difference in behavior between Gaussian and uniform beams concerns the image shift [4.17–4.19], i.e., the difference between the position of the image for Gaussian illumination and its position for uniform illumination, as shown in Fig. 4.4. Comparing Eqs. (3.27) and (4.68), we obtain the image shift as

$$\begin{aligned} \Delta d' = d_g' - d_1' &= -\frac{\dot{H}_f(d)z_R^2}{n_0\left[\dot{H}_a(d) + n_0 d_1 \dot{H}_f(d)\right]\left[\dot{H}_f^2(d)z_R^2 + \left(\dot{H}_a(d) + n_0 d_1 \dot{H}_f(d)\right)^2\right]} \\ &= \frac{1}{2n_0 g^2(d)}\frac{d}{dz}\left\{\ln\left[1 + \frac{\dot{H}_f^2(z)z_R^2}{\left(\dot{H}_a(z) + n_0 d_1 \dot{H}_f(z)\right)^2}\right]\right\}\Bigg|_{z=d} \end{aligned} \tag{4.72}$$

When the waist of the incident Gaussian beam and the point source for uniform illumination are located at the input face of the GRIN lens, that is, when both sources are located at the input, Eq. (4.72) reduces to

$$\begin{aligned} (\Delta d')_{d_1=0} &= -\frac{\dot{H}_f(d)z_{pR}^2}{n_0 \dot{H}_a(d)\left[\dot{H}_f^2(d)z_{pR}^2 + \dot{H}_a^2(d)\right]} = \frac{z_{pR}^2}{n_0^2 l\left[\dot{H}_f^2(d)z_{pR}^2 + \dot{H}_a^2(d)\right]} \\ &= \frac{1}{2n_0 g^2(d)}\frac{d}{dz}\left\{\ln\left[1 + \frac{\dot{H}_f^2(z)z_{pR}^2}{\dot{H}_a^2(z)}\right]\right\}\Bigg|_{z=d} \end{aligned} \tag{4.73}$$

where l is the front working distance for uniform illumination given by Eq. (3.34).

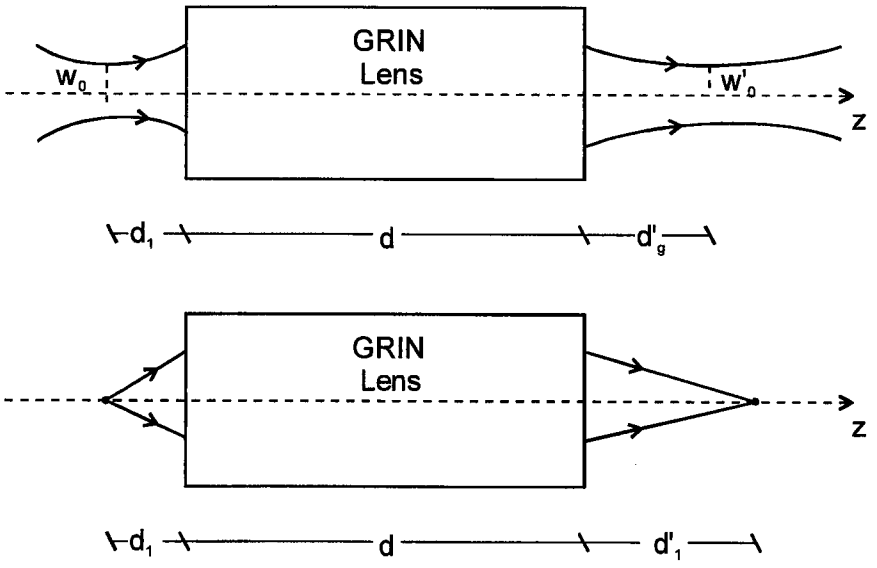

Fig. 4.4. Comparison between Gaussian beam and uniform illumination: image shift.

In the same way, comparing the behavior of a GRIN lens illuminated by a Gaussian plane beam and by a uniform plane wave, the focal shift can be evaluated as shown in Fig. 4.5. From Eqs. (3.10) and (4.71) we can express the focal shift (or the working distance shift) as

$$\Delta l' = l'_g - l' = \frac{\dot{H}_a(d)}{n_0 \dot{H}_f(d)\left[\dot{H}_f^2(d) z_{pR}^2 + \dot{H}_a^2(d)\right]} = -\frac{1}{\left[\dot{H}_f^2(d) z_{pR}^2 + \dot{H}_a^2(d)\right]}$$
$$= \frac{1}{2n_0 g^2(d)} \frac{d}{dz}\left\{\ln\left[z_{pR}^2 + \frac{\dot{H}_a^2(z)}{\dot{H}_f^2(z)}\right]\right\}\Bigg|_{z=d} \tag{4.74}$$

By comparing Eqs. (4.73–4.74), we have

$$\frac{(\Delta d')_{d_1=0}}{\Delta l'} = -\left(\frac{z_{pR}}{n_0 l}\right)^2 = -\left(\frac{\pi w_0^2}{l\lambda}\right)^2 \tag{4.75}$$

where Eq. (4.18) has been used.

Thus, the relationship between the image shift at $d_1 = 0$ and the focal shift is proportional to the square of the ratio between the square of the waist of the Gaussian beam and the front working distance of the GRIN lens.

It is essential to know image and focal shifts for optimized performance of devices such as optical GRIN connectors illuminated with Gaussian beams. Any deviation from position of the image of the back focus has the effect of reducing the efficiency of coupling, there by adding insertion losses to the device.

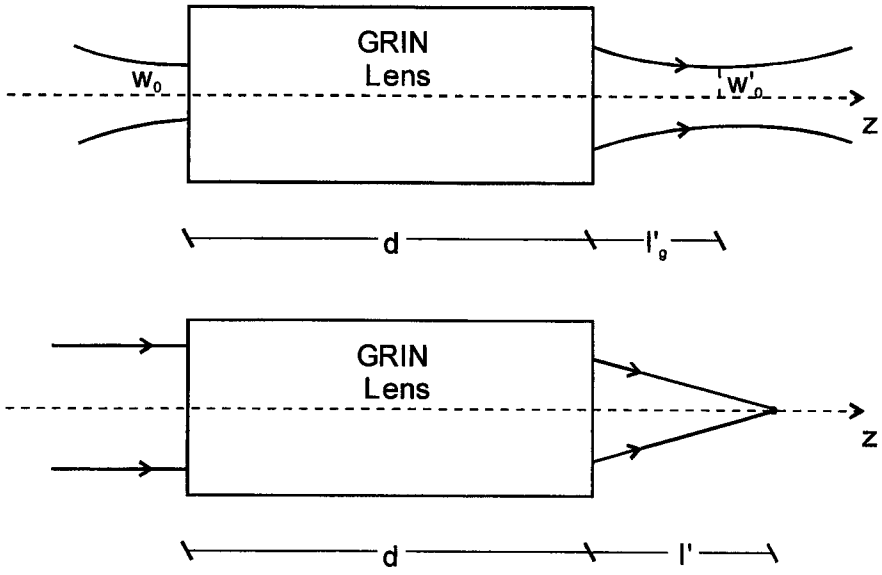

Fig. 4.5. Comparison between Gaussian and uniform plane waves: focal shift.

Another example of the difference in behavior between Gaussian beams and uniform waves occurs when the waist of the incident beam is at the front focal plane of the GRIN lens, in which case the emerging beam has a waist at the back focal plane. The position of the front focal plane measured from the input face of the GRIN lens for uniform illumination is given by Eq. (3.34). When the input waist is located at this plane, $d_1 = l$, the output waist is at the back focal plane, that is

$$d'_g = -\frac{H_f(d)}{n_0 \dot{H}_f(d)} = l' \tag{4.76}$$

where Eqs. (3.33) and (4.68) has been used.

To evaluate image and focal shifts we apply the above results to the selfoc lens, since this kind of lens is used mainly as a GRIN connector in devices for optical communications. In this case, the axial and field rays are given by Eqs. (1.96).

With Eqs. (1.96) inserted into Eqs. (4.72–4.74) and $g(d) = g_0$, image and focal shifts become

$$\Delta d' = \frac{w^4(0)/w_{fm}^4}{n_0 g_0 \sin^2(g_0 d)[\operatorname{cotan}(g_0 d) - n_0 g_0 d_1]\left[\dfrac{w^4(0)}{w_{fm}^4} + (\operatorname{cotan}(g_0 d) - n_0 g_0 d_1)^2\right]} \tag{4.77}$$

$$(\Delta d')_{d_1=0} = \frac{w_0^4 / w_{fm}^4}{n_0 g_0 \cot(g_0 d)\sin^2(g_0 d)\left[\frac{w_0^4}{w_{fm}^4} + \cot^2(g_0 d)\right]} \tag{4.78}$$

$$\Delta l' = -\frac{1}{n_0 g_0 \tan(g_0 d)\sin^2(g_0 d)\left[\frac{w_0^4}{w_{fm}^4} + \cot^2(g_0 d)\right]} \tag{4.79}$$

where Eqs. (4.14) and (4.18) have been used, and w_{fm} is the waist radius of the fundamental mode in a selfoc lens given by Eq. (4.47).

Note that when $w_{fm} = w(0)$ or $w_{fm} = w_0$, Eqs. (4.77–4.79) reduce to

$$\Delta d' = \frac{1}{n_0 g_0 \sin^2(g_0 d)[\cot(g_0 d) - n_0 g_0 d_1][1 + (\cot(g_0 d) - n_0 g_0 d_1)^2]} \tag{4.80}$$

$$(\Delta d')_{d_1=0} = \frac{1}{n_0 g_0 \cot(g_0 d)} = -d_1'|_{d_1=0} \tag{4.81}$$

$$\Delta l' = -\frac{1}{n_0 g_0 \tan(g_0 d)} = -l' \tag{4.82}$$

Equations (4.81–4.82) give the image position and the back working distance for uniform illumination, and they indicate once again the adiffractional behavior of light propagation inside the GRIN lens for $w_{fm} = w_0$.

Figure 4.6a shows the variation of image shift against normalized thickness $g_0 d$ for $w(0) \le w_{fm}$ and $w(0) \rangle\rangle w_{fm}$, and for object distance $d_1 = 100\,\mu m$. Note that when

$$d_1 = \frac{\cot(g_0 d)}{n_0 g_0} \tag{4.83}$$

that is, when the object distance is equal to the front working distance given by Eq. (3.34) the image shift goes to infinity, since for uniform illumination $d_1' \to \infty$, and for Gaussian illumination $d_g' = \cos(g_0 d) / n_0 g_0$.

Figure 4.6 depicts focal shift versus $g_0 d$ for $w(0) \le w_{fm}$ and $w(0) \rangle\rangle w_{fm}$. In both figures $\lambda = 1.56\,\mu m$. Selfoc lens data correspond to a w–type selfoc microlens with diameter of 2 mm [4.20].

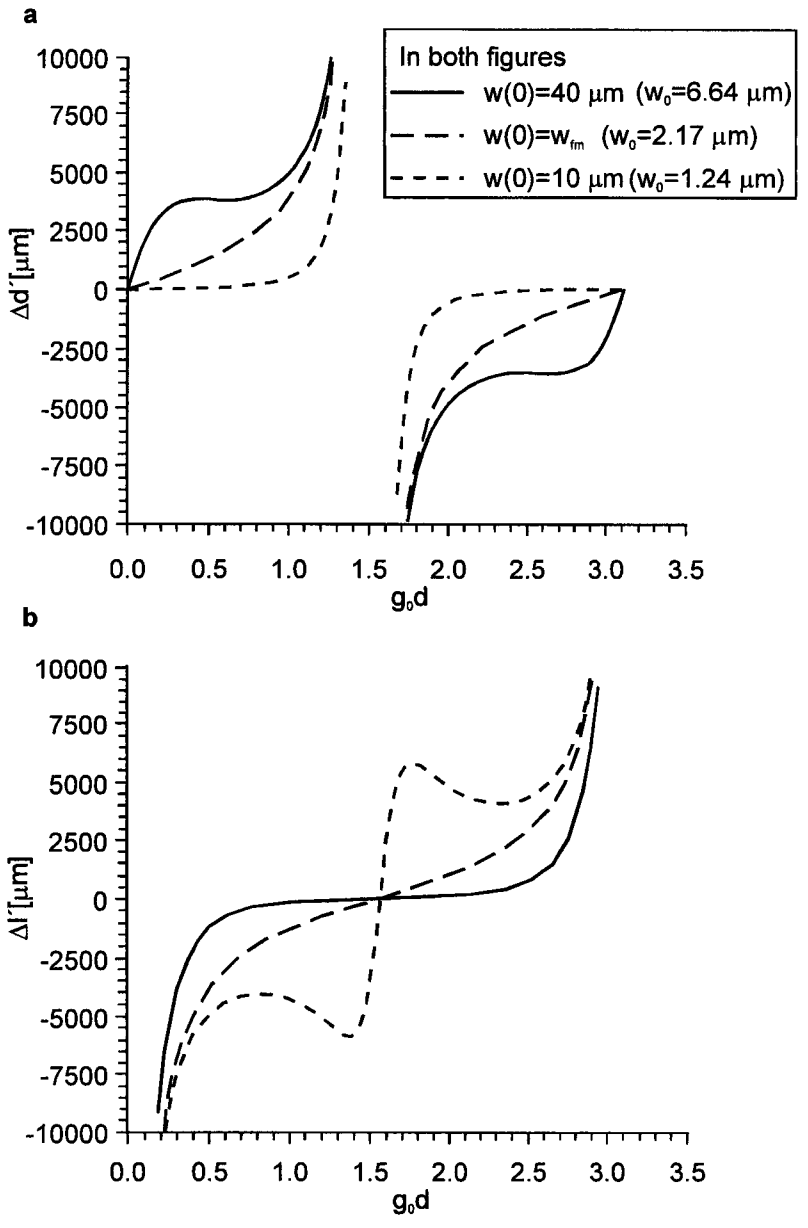

Fig. 4.6. Variation of **a** image and **b** focal shifts with normalized thickness of selfoc lens. Calculations have been made for $d_0 = 100\,\mu m$ (in a), $\lambda = 1.56\,\mu m$, $w_{fm} = 23.04\,\mu m$, $n_0 = 1.59$, and $g_0 = 0.294\,mm^{-1}$.

4.4 Effective Aperture

Until now we have not considered the finite cross–section of the GRIN lens; we shall now study the effect of this limitation on Gaussian beam propagation through a GRIN lens of radius a and thickness d. A spherical Gaussian beam will be confined in a GRIN lens if the following condition is satisfied

$$\frac{w(z)}{|G(z)|_M} \leq a \tag{4.84}$$

where $|G(z)|_M$ denotes the maximum value of $|G(z)|$ in the lens.

Equation (4.84) indicates that it will be necessary to define the effective aperture a_e of the input face of the GRIN lens (Fig. 4.7) since not all the Gaussian beam reaching the lens will be confined through it.

From Eq. (4.84) it follows that the effective aperture of the input face of the GRIN lens is given by

$$a_e = \frac{w(0)}{|G(z)|_M} \tag{4.85}$$

where Eq. (4.13) has been used.

The evolution of a_e for ray confinement inside the GRIN lens can be written as

$$a_e(z) = a_e|G(z)| \tag{4.86}$$

verifying

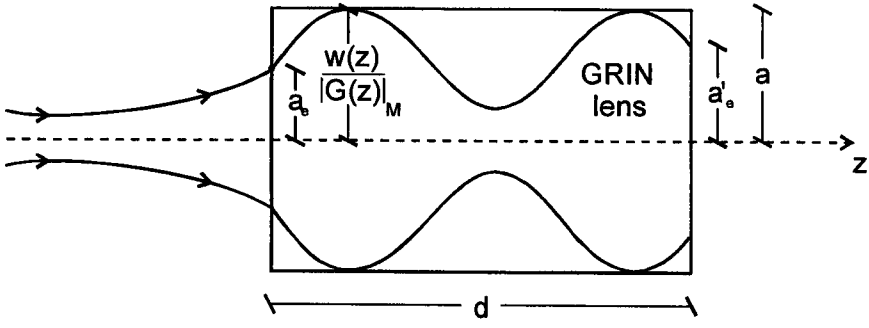

Fig. 4.7. Geometry for evaluating the effective aperture of a GRIN lens illuminated by a Gaussian beam.

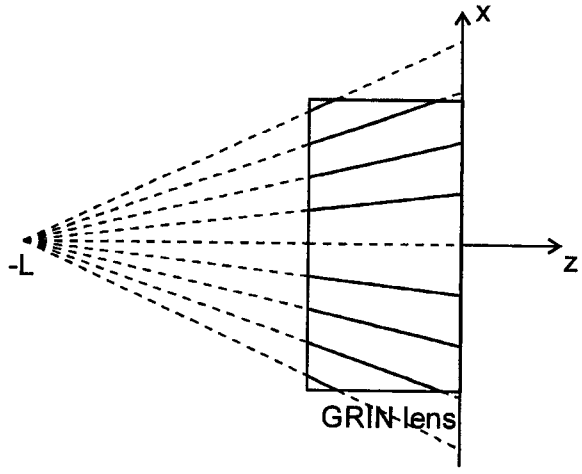

Fig. 4.8. Equi-index cones for a GRIN lens with divergent linear taper function.

$$0 \le a_e(z) \le a \tag{4.87}$$

Then the effective aperture for the output face of the GRIN lens will be given by

$$a_e' = a_e|G(d)| \tag{4.88}$$

As mentioned in Sect. 4.2, $|G(z)|_M$ is obtained for $u(z^+)$ as $w_{fm}(0) \ge w(0)$ or $w_{fm}(0) \langle w(0)$ and $R(0) \rangle 0$, and for $u(z^-)$ as $w_{fm}(0) \ge w(0)$ or $w_{fm}(0) \langle w(0)$ and $R(0) \langle 0$.

For the sake of simplicity, we suppose an incident Gaussian beam that has its waist located on the input face of the GRIN lens. In other words, for the lens illuminated by a plane Gaussian beam, $R(0) \to \infty$, $w(0) \to w_0$ and Eqs. (1.92), (4.15), and (4.56–4.60) provide

$$|G_p(z^+)|_M = \frac{g_0 w_{fm}^4(0)}{g(z^+) w_0^4} \quad \text{when} \quad w_{fm}(0) \rangle w_0 \tag{4.89}$$

$$|G_p(z^-)|_M = \frac{g_0}{g(z^-)} \quad \text{when} \quad w_{fm}(0) \langle w_0 \tag{4.90}$$

and

$$|G_p(z)|_M = \frac{g_0}{g(z)} \quad \text{when} \quad w_{fm}(0) = w_0 \tag{4.91}$$

for all values of z inside the GRIN lens.

We can apply these results to a GRIN lens with a divergent linear taper function given by [4.21]

$$g(z) = \frac{g_0}{1 + z/L} \tag{4.92}$$

where g_0 is the value of g(z) at the input face of the GRIN lens, and L is the distance from this face to the common apex of the equi–index cones (Fig. 4.8).

In this kind of GRIN lens, axial and field rays are given by

$$H_a(z) = \frac{1}{g_0}\left(1 + \frac{z}{L}\right)^{1/2} \sin\left[g_0 L \ln\left(1 + \frac{z}{L}\right)\right] \tag{4.93}$$

$$H_f(z) = \left(1 + \frac{z}{L}\right)^{1/2} \cos\left[g_0 L \ln\left(1 + \frac{z}{L}\right)\right] \tag{4.94}$$

For plane Gaussian illumination, the axial positions in which |G| is maximum as $w_{fm}(0) < w_0$ or $w_{fm}(0) > w_0$ can be expressed, respectively, as

$$z_m^+ = L\left[e^{\frac{(2m+1)\pi}{2g_0 L}} - 1\right] \tag{4.95}$$

$$z_m^- = L\left[e^{\frac{m\pi}{g_0 L}} - 1\right] \tag{4.96}$$

where m is an integer. The first maximum value of G is obtained for m = 0, the second one for m = 1, and so on.

From Eqs. (4.95–4.96) it follows that

$$|G_p(z^+)|_M = \frac{w_{fm}^4(0)}{w_0^4} e^{\frac{(2m+1)\pi}{2g_0 L}} \quad \text{when} \quad w_{fm}(0) \rangle w_0 \tag{4.97}$$

$$|G_p(z^-)|_M = e^{\frac{m\pi}{g_0 L}} \quad \text{when} \quad w_{fm}(0) \langle w_0 \tag{4.98}$$

and

$$|G_p(z)|_M = \frac{L + z}{L} \quad \text{when} \quad w_{fm}(0) = w_0 \tag{4.99}$$

for all values of z.

Thus, the evolution of the effective aperture inside the GRIN lens is given by

$$a_e(z) = \frac{w_0^5}{w_{fm}^4(0)} |G(z)| e^{-\frac{(2m+1)\pi}{2g_0 L}} \quad \text{when} \quad w_{fm}(0) > w_0 \tag{4.100}$$

$$a_e(z) = w_0 |G(z)| e^{-\frac{m\pi}{g_0 L}} \quad \text{when} \quad w_{fm}(0) < w_0 \tag{4.101}$$

and

$$a_e(z) = \frac{L}{L+z} w_{fm}(z) \quad \text{when } w_{fm}(0) = w_0 \tag{4.102}$$

Finally, the results obtained in this chapter can be extended to GRIN lenses illuminated by Gaussian beams with two complex curvatures (elliptical Gaussian beams). Likewise, the diffractive effect due to finite aperture (diffraction–limited propagation of light) can also be evaluated, in the same way as in Chap. 3, by Lommel functions with complex arguments [4.22].